

secreted by transfected COS or Chinese hamster ovary cells begins at a glycine residue at position 21; the non-glycosylated form has a molecular mass of 12,397 by electrospray mass spectrometry, close to the predicted  $M_r$  of 12,399, although it migrates as a 9K protein on SDS-PAGE (Fig. 1C).

The production by monocytes of inflammatory cytokines such as IL-1, IL-6 and tumour necrosis factor- $\alpha$  (TNF- $\alpha$ ) is a crucial initiating event in a number of infectious and inflammatory pathologies. We have found that IL-13 strongly inhibits IL-6 secretion induced by bacterial lipopolysaccharide (LPS) in peripheral blood mononuclear cells (PBMC) (Fig. 3a). IL-13 would appear to be acting directly on monocytes because an inhibition of IL-6 mRNA accumulation is observed rapidly (within 4 hours) in cultures of PBMC enriched in monocytes by adherence to tissue culture dishes (Fig. 3b). A marked inhibition is also seen for other inflammatory monokine mRNAs (IL-1 $\beta$ , TNF- $\alpha$ , IL-8, gro- $\beta$ ) in LPS-treated monocytes in the presence of IL-13 (Fig. 3b, and other data not shown). The action of IL-13 would thus seem to be a generalized block on inflammatory monokine synthesis, a property shared with the other Th2 lymphokines IL-4 and IL-10 (ref. 13). IL-13 and IL-4 show similar levels of inhibition of IL-6 synthesis (Fig. 3a). IL-13 also inhibits production of human immunodeficiency virus (HIV) by tissue-culture differentiated macrophages<sup>14</sup>, contrasting with the stimulatory effects of macrophage-activating cytokines such as IL-3 and GM-CSF on HIV production that have been reported in comparable conditions<sup>15</sup>.

The production of IFN- $\gamma$  by large granular lymphocytes (LGL) may direct subsequent immune responses, leading to macrophage activation and to a 'Th1-type' cellular immune response<sup>16</sup>. The major cytokine influencing this production of IFN- $\gamma$  is IL-2 (ref. 17). We have found that IL-13 has a small, direct effect on IFN- $\gamma$  synthesis by LGL, and synergizes with both suboptimal and optimal doses of IL-2 (Fig. 3c). In this respect it resembles IL-12 (ref. 17), rather than IL-4, which strongly inhibits IFN- $\gamma$  synthesis by these cells (Fig. 3c).

IL-13 also affects B lymphocytes, increasing their proliferation and the expression of the CD23 surface antigen (P. Carayon and T. Defrance, personal communication). IL-13 is thus a highly pleiotropic cytokine. In its anti-inflammatory effects on monocytes and its stimulation of the humoral response through B lymphocytes, IL-13 contributes to the 'Th2-type' response together with IL-4 and IL-10 (refs 18, 19). In, however, its effects on IFN- $\gamma$  synthesis, it might be expected to promote a 'Th1-type' cellular immune response<sup>16,20</sup>. A full understanding of the cytokine network in different pathological situations now needs to take into account the activities of IL-13.

The anti-inflammatory function of IL-13 may be crucial in clinical inflammation, for example in septic shock<sup>21</sup> or rheumatoid arthritis<sup>22</sup>. Its activity on LGL may be clinically interesting in that, unlike IL-4, it does not decrease and can even increase the IL-2-induced lymphokine-activated killer activity of these cells (our unpublished results). As IL-13 also inhibits HIV replication *in vitro*<sup>14</sup>, and systemic immunity to parental tumour cells can be induced by IL-13-secreting tumour cells *in vivo* (D. Fradelizi, personal communication), IL-13 would appear to represent a potentially important new member of the therapeutic cytokine arsenal. □

Received 15 December 1992; accepted 25 February 1993.

- Linsley, P. S., Clark, E. A. & Ledbetter, J. A. *Proc. natn. Acad. Sci. U.S.A.* **87**, 5031-5035 (1990).
- Gimmi, C. D. *et al. Proc. natn. Acad. Sci. U.S.A.* **88**, 6575-6579 (1991).
- Thompson, C. B. *et al. Proc. natn. Acad. Sci. U.S.A.* **86**, 1333-1337 (1989).
- Morgan, J. G., Dolganov, G. M., Robbins, S. E., Hinton, L. M. & Lovett, M. *Nucleic Acids Res.* **20**, 5173-5179 (1992).
- Kozak, M. *Nucleic Acids Res.* **12**, 857-872 (1984).
- von Heijne, G. *Nucleic Acids Res.* **14**, 4683-4690 (1986).
- Caput, D. *et al. Proc. natn. Acad. Sci. U.S.A.* **83**, 1670-1674 (1986).
- Shaw, G. & Kamen, R. *Cell* **46**, 659-667 (1986).
- Powers, R. *et al. Science* **256**, 1673-1677 (1992).
- Morrison, B. W. & Leder, P. *J. biol. Chem.* **267**, 11957-11963 (1992).
- Brown, K. D., Zurawski, S. M., Mosmann, T. R. & Zurawski, G. *J. Immunol.* **142**, 679-687 (1989).

- Cherwinski, H. M., Schumacher, J. H., Brown, K. D. & Mosmann, T. R. *J. exp. Med.* **166**, 1229-1244 (1987).
- de Waal Malefyt, R., Abrams, J., Bennett, B., Figdor, C. G. & de Vries, J. E. *J. exp. Med.* **174**, 1209-1220 (1991).
- Montaner, L. J. *et al. J. Cell. Biochem. Abstr. suppl.* **17B**, 94 (1993).
- Koyanagi, Y. *et al. Science* **241**, 1673-1675 (1988).
- Scott, P. *J. Immunol.* **147**, 3149-3155 (1991).
- Kobayashi, M. *et al. J. exp. Med.* **170**, 827-845 (1989).
- Boom, W. H., Liano, D. & Abbas, A. K. *J. exp. Med.* **167**, 1350-1363 (1988).
- Zlotnik, A. & Moore, K. *Cytokine* **3**, 366-371 (1991).
- Cher, D. J. & Mosmann, T. R. *J. Immunol.* **138**, 3688-3694 (1987).
- Ohlsson, K., Bjork, P., Bergenfeldt, M., Hageman, R. & Thompson, R. C. *Nature* **348**, 550-552 (1990).
- Williams, R. O., Feldmann, M. & Maini, R. N. *Proc. natn. Acad. Sci. U.S.A.* **89**, 9784-9788 (1992).
- Seed, B. & Aruffo, A. *Proc. natn. Acad. Sci. U.S.A.* **84**, 3365-3369 (1987).
- Dermer, A. J., Bole, D. G. & Kaufman, R. J. *J. cell. Biol.* **105**, 2665-2674 (1987).
- Devereux, J., Haerberli, P. & Smithies, O. *Nucleic Acids Res.* **12**, 387-395 (1984).
- Aarden, L. A., DeGroot, E. R., Schapp, O. L. & Lansdorp, P. M. *Eur. J. Immunol.* **17**, 1411-1416 (1987).
- Brake, A. J. *Meth. Enzym.* **185**, 408-421 (1990).
- Timonen, T., Reynolds, C. W., Ortaldo, J. R. & Herberman, R. B. *J. Immunol. Meth.* **51**, 269-277 (1982).

ACKNOWLEDGEMENTS. We thank B. and M. Delpach, M. Goncalves and M. F. Jamme for technical assistance, P. Carayon, M. Magazin, B. Pessegue, and N. Vita for discussion, and P. Ramond for help and advice on DNA sequence comparison.

## Correction of the ion transport defect in cystic fibrosis transgenic mice by gene therapy

Stephen C. Hyde, Deborah R. Gill,  
Christopher F. Higgins\* & Ann E. O. Trezise

Imperial Cancer Research Fund Laboratories, Institute of Molecular Medicine, University of Oxford, John Radcliffe Hospital, Oxford OX3 9DU, UK

Lesley J. MacVinish & Alan W. Cuthbert

Department of Pharmacology, University of Cambridge, Tennis Court Road, Cambridge CB2 1QJ, UK

Rosemary Ratcliff, Martin J. Evans  
& William H. Colledge

Wellcome/CRC Institute of Cancer and Developmental Biology and Department of Genetics, University of Cambridge, Tennis Court Road, Cambridge CB2 1QR, UK

**CYSTIC FIBROSIS (CF) is a lethal inherited disorder affecting about 1 in 2,000 Caucasians. The major cause of morbidity is permanent lung damage resulting from ion transport abnormalities in airway epithelia that lead to mucus accumulation and bacterial colonization. CF is caused by mutations in the cystic fibrosis transmembrane conductance regulator (CFTR) gene<sup>1</sup> that encodes a cyclic-AMP-regulated chloride channel<sup>2,3</sup>. Cyclic-AMP-regulated chloride conductances are altered in airway epithelia from CF patients<sup>4-6</sup>, suggesting that the functional expression of CFTR in the airways of CF patients may be a strategy for treatment. Transgenic mice<sup>7-9</sup> with a disrupted *cftr* gene are appropriate for testing gene therapy protocols. Here we report the use of liposomes to deliver a CFTR expression plasmid to epithelia of the airway and to alveoli deep in the lung, leading to the correction of the ion conductance defects found in the trachea of transgenic (*cf/cf*) mice. These studies illustrate the feasibility of gene therapy for the pulmonary aspects of CF in humans.**

Plasmid DNA complexed with cationic liposomes can be successfully delivered and expressed in airway epithelia of rodents<sup>10,11</sup>. A suitable plasmid for expressing CFTR protein was constructed in the vector pREP8 (see legend to Fig. 1). In this plasmid, pREP8-CFTR, the human CFTR complementary DNA is under transcriptional control of the constitutive Rous sarcoma virus (RSV) 3' long terminal repeat (LTR) promoter, known to be active in nonproliferating airway epithelial cells<sup>10</sup>. To show that pREP8-CFTR expresses CFTR protein after

\* To whom correspondence should be addressed.

transfection, plasmid DNA complexed with cationic liposomes was introduced into HeLa cells and CFTR protein detected by western blotting (Fig. 1a). To ascertain whether the expressed CFTR protein was functional, cAMP-stimulated iodide efflux was measured in transfected cells (Fig. 1b). In HeLa cells transfected with pREP8-CFTR, iodide efflux was stimulated by a cAMP-agonist cocktail. The cocktail did not stimulate efflux from cells transfected with the vector pREP8. The characteristics of this cAMP-stimulated anion efflux were similar to those reported previously for CFTR-expressing cells<sup>12,13</sup>. Thus, cells transfected with pREP8-CFTR express functional CFTR protein.

RNA *in situ* hybridization was used to demonstrate that the CFTR expression plasmid can be delivered to airway epithelial cells by liposome-mediated transfection *in vivo*. Because CFTR messenger RNA is expressed at high levels in human and rodent intestinal crypts<sup>14-16</sup>, mouse intestinal sections were used as controls to demonstrate probe specificity. No hybridization to mouse intestine was detected with either of two human CFTR probes whereas, in consecutive sections, the mouse antisense *cftr* probe (but not the sense probe) detected abundant *cftr* mRNA in the crypts (data not shown). Additionally, neither the antisense nor the sense *hisD* vector control probes hybridized with mouse intestinal mRNA, as expected (data not shown). This demonstrates that the human CFTR and vector *hisD* probes do not cross-hybridize with mouse *cftr* mRNA.

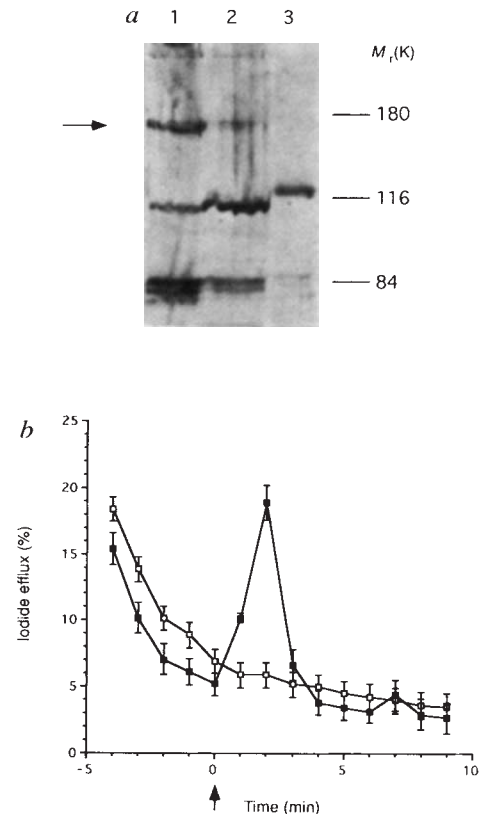
After transfection of pREP8-CFTR DNA into the airways of mice of 20-28 days old, sequences corresponding to human CFTR were detected by *in situ* hybridization (Fig. 2). Strong hybridization signals were observed in isolated groups of airway cells using both the human CFTR probe (Fig. 2a-c) and the

*hisD* vector-specific probe (d-f). In a series of consecutive sections the hybridization signals observed with the human CFTR and *hisD* probes colocalized to the same airways and airspaces (Fig. 2a-f). No hybridization was detected with the mouse *cftr* probe. This provides strong evidence that the hybridization signals obtained are highly specific and due to the transfected plasmid. Hybridization of these same probes to lung sections from untransfected animals served as a negative control against nonspecific hybridization; neither the human CFTR probe (g-i) nor the *hisD* probe (j-l) hybridized to any mRNAs in the lungs of untransfected mice. Hybridization signals were obtained with both the sense and antisense probes (Fig. 2a-f). Normally the antisense probe is used to detect mRNA whereas the sense probe serves as a negative control. Following transfection, however, both the sense and antisense probes would be expected to recognize vector DNA. The stronger signal observed with the antisense probe indicates transcription. This was seen for the *hisD* gene which is transcribed from a vector promoter. In most hybridizing cells, the signal obtained with the antisense human CFTR probe (Fig. 2b) was also greater than that obtained with the sense probe (c), implying that human CFTR mRNA is expressed following transfection.

The data in Fig. 3 show hybridization to sections through different regions of the lungs of a mouse which had been transfected with pREP8-CFTR. No expression of endogenous mouse *cftr* mRNA was detected in any region of the lung (data not shown), consistent with previous studies showing low-level *cftr* expression in rodent lung<sup>14</sup>, and with detailed studies of these transgenic animals (A.E.O.T. *et al.*, manuscript in preparation). This shows that the transfection protocol does not induce expression of endogenous mouse *cftr* mRNA. Human CFTR

FIG. 1 Expression of functional CFTR protein from plasmid pREP8-CFTR in HeLa cells. a, Western blot confirming expression of CFTR after transfection of HeLa cells using Lipofectin. Lanes 1, HT29 cells; 2, HeLa cells transfected with pREP8-CFTR; 3, HeLa cells transfected with the vector pREP8. The HT29 cells served as a positive control for CFTR expression and migration<sup>25,26</sup>, indicated by the arrow. The ~115 and 85K bands are due to nonspecific cross reactions of the antibody<sup>25</sup>.  $M_r \times 1,000$  of markers is indicated. b, Time course of iodide efflux from HeLa cells. Cells were transfected with plasmid pREP8-CFTR (■) or the vector pREP8 (□). The arrow indicates the point at which a cAMP-agonist cocktail was added. The data are displayed as the mean of three individual experiments ( $\pm$ s.e.m.), expressed as a percentage of the total efflux.

**METHODS.** Human CFTR cDNA encoding the entire CFTR coding sequence<sup>1</sup> (nucleotides 133-4,620) was inserted into the plasmid pREP8 (Invitrogen), under transcriptional control of the RSV 3' LTR promoter, to create plasmid pREP8-CFTR. The cDNA incorporated three minor changes from the published sequence (C to G at nucleotide 136<sup>13</sup>; T to C at nucleotide 936<sup>27</sup>; A to C at nucleotide 1990<sup>28</sup>), and included a Kozak translation initiation sequence<sup>29</sup> (CCACCATG) immediately 5' to the translation initiation codon. For plasmid transfection,  $1 \times 10^6$  HeLa cells were seeded into each well of 35-mm, 6-well tissue culture dishes in Dulbecco's modified Eagles medium supplemented with 10% fetal calf serum, and incubated at 37 °C. After 24 h growth, cells in each well were transfected with 8  $\mu$ g plasmid DNA mixed with 13  $\mu$ g Lipofectin (Gibco BRL) and diluted to 3 ml in Optimum 1 (Gibco BRL). After a further 24-48-h incubation at 37 °C, cells were either collected for protein extraction or used for anion efflux measurements. For protein extraction, cells were washed five times with ice-cold PBS and collected into a buffer containing 10 mM Tris-Cl pH 8.0, 10 mM KCl, 1.5 mM MgCl<sub>2</sub>, and the protease inhibitors antipain (50  $\mu$ g ml<sup>-1</sup>), aprotinin (10  $\mu$ g ml<sup>-1</sup>), benzamide (310  $\mu$ g ml<sup>-1</sup>), leupeptin (5  $\mu$ g ml<sup>-1</sup>), pepstatin A (5  $\mu$ g ml<sup>-1</sup>) and phenylmethylsulphonyl fluoride (175  $\mu$ g ml<sup>-1</sup>). Cells were lysed by repeated passage through a 19-gauge needle. Cellular and nuclear debris were removed from the lysate by a 5-min centrifugation at 300g and membranes pelleted by a 30-min centrifugation at 100,000g. The membrane pellet was dissolved in 2.5% Triton X-100 and separated by electrophoresis on a 6% SDS-polyacrylamide gel. CFTR was detected by western blotting after transfer to a Hybond C-super membrane (Amersham) using the well characterized anti-CFTR antisera 181<sup>25</sup>. Immunodetection was by enhanced chemiluminescence (ECL; Amersham). To measure cAMP-stimulated efflux, the transfected cells were preloaded with iodide by incubation for 40 min at room temperature in 3 ml loading buffer (136 mM NaI, 3 mM KNO<sub>3</sub>, 2 mM Ca(NO<sub>3</sub>)<sub>2</sub>, 11 mM glucose, 20 mM HEPES, pH 7.4). Extracellular NaI was removed by



6  $\times$  1 ml rinses in efflux buffer (loading buffer with 136 mM NaNO<sub>3</sub> replacing the NaI). Cells were then washed with 1 ml efflux buffer for 1 min using a sample-replace procedure. After the fifth 1-min sample (designated time 0), cAMP-agonists (1 mM 3-isobutyl-1-methylxanthine (IBMX), 200  $\mu$ M dibutyryl-cAMP, 10  $\mu$ M forskolin, dissolved in DMSO) were included in the efflux buffer. The concentration of iodide in each 1-ml aliquot was determined using an iodide-specific electrode (HNU systems).

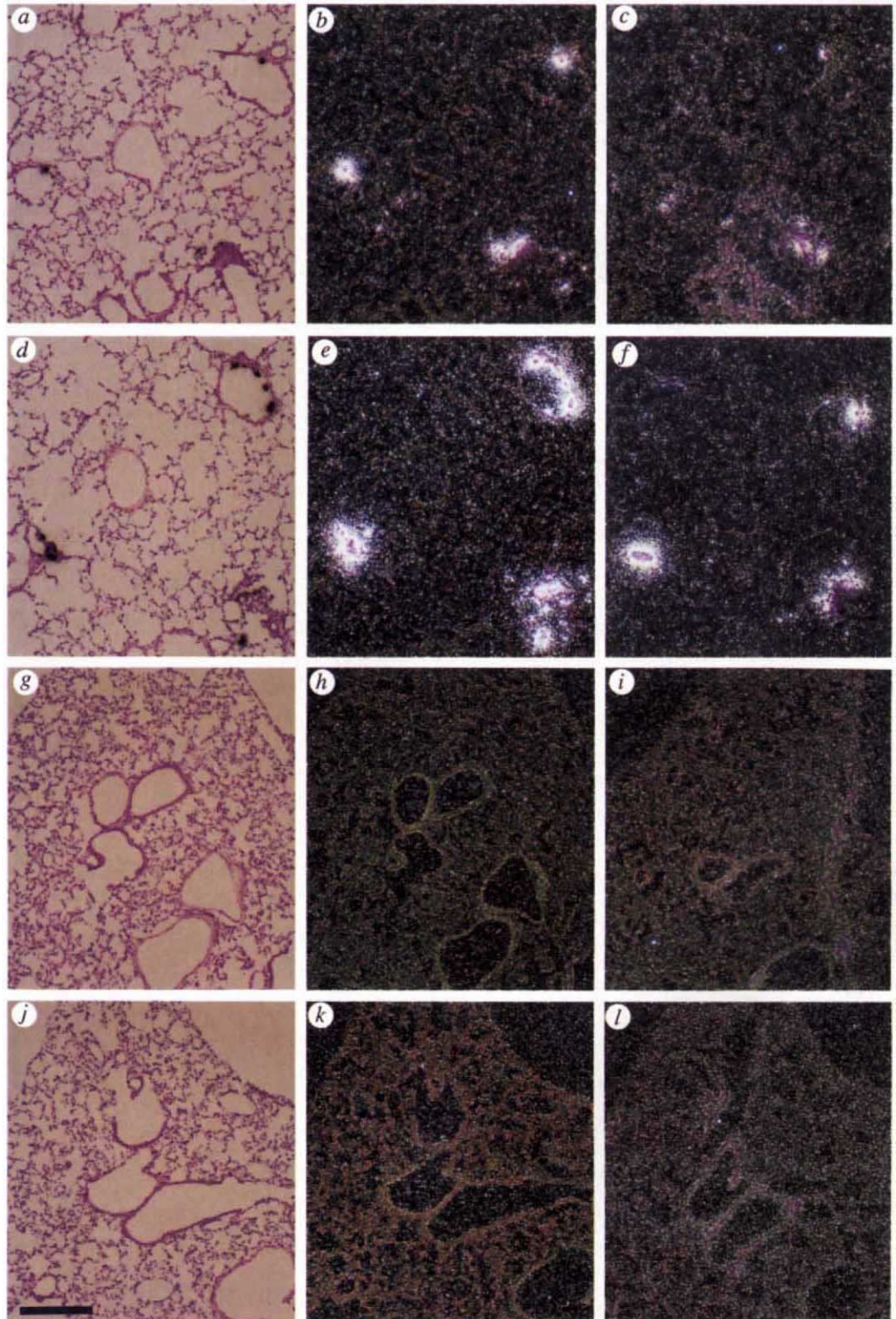
expression was seen in the airways of three out of four animals transfected with pREP8-CFTR and, in at least one transfected animal, human *CFTR* sequences were detected in all five lobes of the lung. Positive cells were detected in large and small airways (Fig. 2*a-d*), and in cells lining the air spaces of the more distal regions of the lung (*e-j*). It appeared to be the surface epithelial cells of the airways that had been transfected. Colocalization of the *CFTR* signal with the *hisD* probe (Fig. 2), confirmed that the signal was a consequence of transfection.

**FIG. 2** Detection of human *CFTR* by *in situ* hybridization in mouse airways following *in vivo* transfection. *a-f*, Data obtained for a mouse transfected with pREP8-CFTR; *g-l*, controls for an untransfected mouse. The probes used were against human *CFTR* exons 1-6 (*a-c* and *g-i*) or the *hisD* vector sequences (*d-f* and *j-l*). For each example, three panels are shown: (1) a brightfield view of a section hybridized with the antisense probe, to illustrate tissue morphology (*a, d, g, j*); (2) a darkfield view of the same section (*b, e, h, k*); (3) a darkfield view of an adjacent section probed with the control sense probe (*c, f, i, l*). Scale bar, 200  $\mu$ m. Similar results were obtained with several animals.

**METHODS.** Mice were given enough avertin by intraperitoneal injection to induce very light anaesthesia. For transfection, ~100  $\mu$ g plasmid DNA was mixed with 25  $\mu$ g Lipofectin in a total volume of 50  $\mu$ l and administered to mice by tracheal instillation in two loads by insertion of a metal applicator, adapted from a 25-gauge blunted syringe needle, through the mouth and into the trachea to the point where the main bronchi branch off. The animals used weighed between 5 g and 12 g. Four days after transfection, *in situ* hybridization was performed on perfusion-fixed tissue by a modification of the method described by Simmons *et al.*<sup>30</sup>, as described previously<sup>15</sup>. <sup>35</sup>S-labelled RNA probes were synthesized *in vitro* by run-off transcription from plasmid DNA, incorporating [<sup>35</sup>S]UTP. The antisense and sense (control) probes were derived from opposite strands of the same plasmid. The plasmids used for probe generation were as follows. The two human *CFTR* probes, corresponding to nucleotides 62-645 (exons 1-6) and nucleotides 1,977-2,461 (exon 13) (numbering according to ref. 1), have been described previously<sup>16</sup>. The mouse *cftr* probes were derived by reverse transcriptase PCR from mouse testis mRNA and corresponded to nucleotides 305-691 of exons 3-5. The *hisD* vector probe was subcloned from pREP8 and corresponded to nucleotides 3,167-3,851. All probes were cloned into Bluescript vectors (Stratagene). After developing,

Thus, transfection is effective and expression of human *CFTR* throughout the airway was achieved.

To determine whether delivery of *CFTR* cDNA to the airways could correct the ion transport defects apparent in CF, we used a recently developed mouse model<sup>9,17</sup>. These transgenic (*cf/cf*) mice are homozygous for a null mutation in *cftr* and express little or no detectable endogenous *cftr* mRNA (A.E.O.T. *et al.*, manuscript in preparation). *CFTR*-dependent, cAMP-stimulated chloride conductances are greatly reduced in the airways



sections were counterstained with haematoxylin and eosin and photographed using a Nikon Microphot FX microscope.

and caeca of these mice, compared with normal (+/+) animals, mimicking features of the human disorder<sup>17</sup>. The mice frequently die shortly after birth as a consequence of intestinal blockages<sup>9</sup>. Ion transport in the trachea was measured by voltage clamping at zero potential, using pharmacological agents to eliminate or stimulate various processes (Fig. 4). Measurements were also made with the caecum of the same animal as an internal control. Figure 4A shows a set of typical results, and Fig. 4B a compilation of the data. For each tracheal preparation, three measurements were made: amiloride-sensitive sodium absorption (labelled  $\text{Na}^+$ ), cAMP-stimulated chloride secretion (labelled  $\text{Cl}^-$  cAMP), and  $\text{Ca}^{2+}$ -stimulated chloride secretion (labelled  $\text{Cl}^-$   $\text{Ca}^{2+}$ ). As expected, CFTR-dependent, cAMP-stimulated

chloride secretion was significantly reduced ( $P < 0.01$ ) in both the tracheas and caeca of the *cf/cf* mice compared with the normal (+/+) mice. There was no significant difference in the cAMP-stimulated chloride secretion between untreated and pREP8-transfected normal mice, indicating that transfection itself has no effect on ion transport. Most importantly, transfection of *cf/cf* mice with pREP8-CFTR restored the cAMP-stimulated chloride secretion in the trachea to a level comparable with that of normal (+/+) animals. In sharp contrast, transfection of the *cf/cf* mice with the vector pREP8 had no significant effect on the cAMP-stimulated chloride secretion in the trachea. The caecum of *cf/cf* mice transfected with pREP8-CFTR showed no appreciable cAMP-stimulated chloride secretion

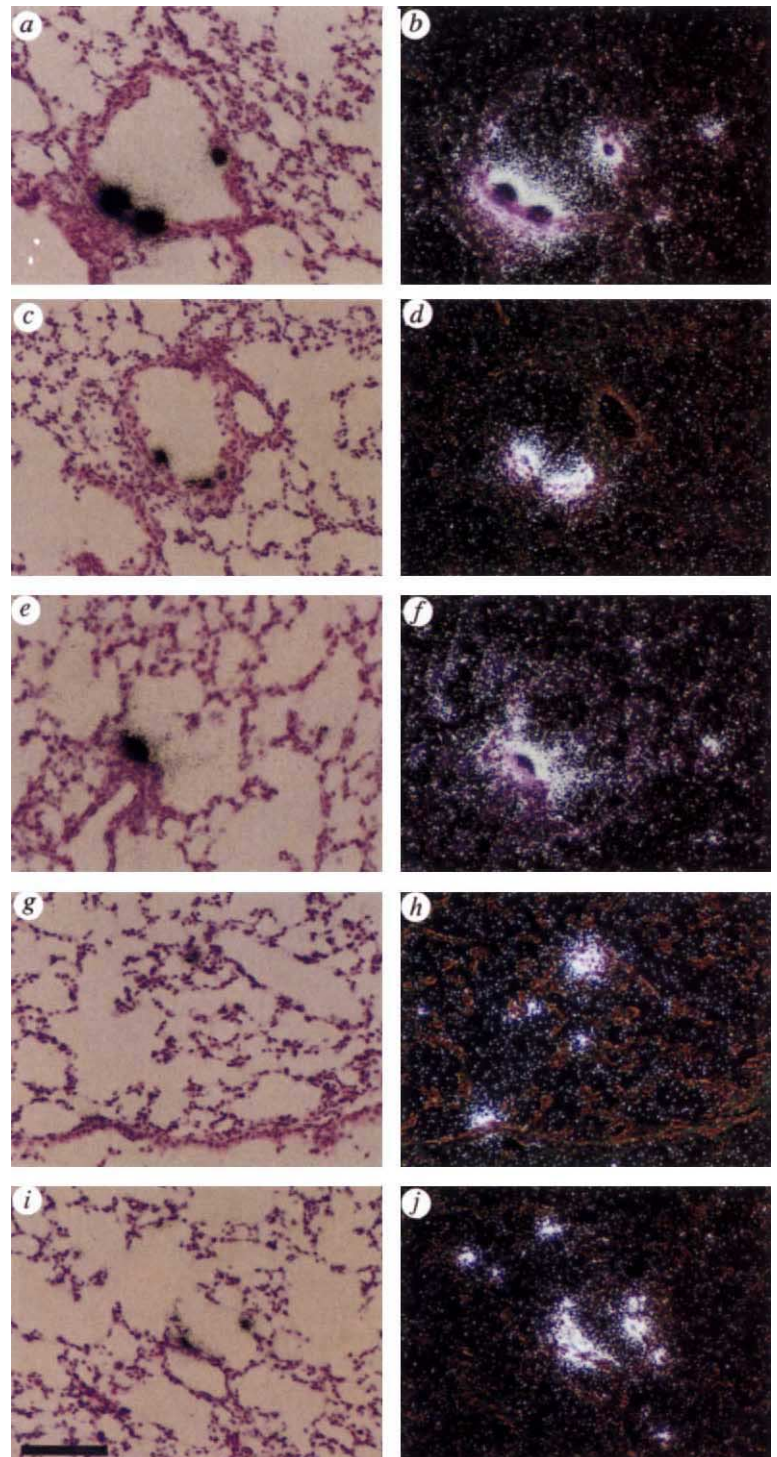
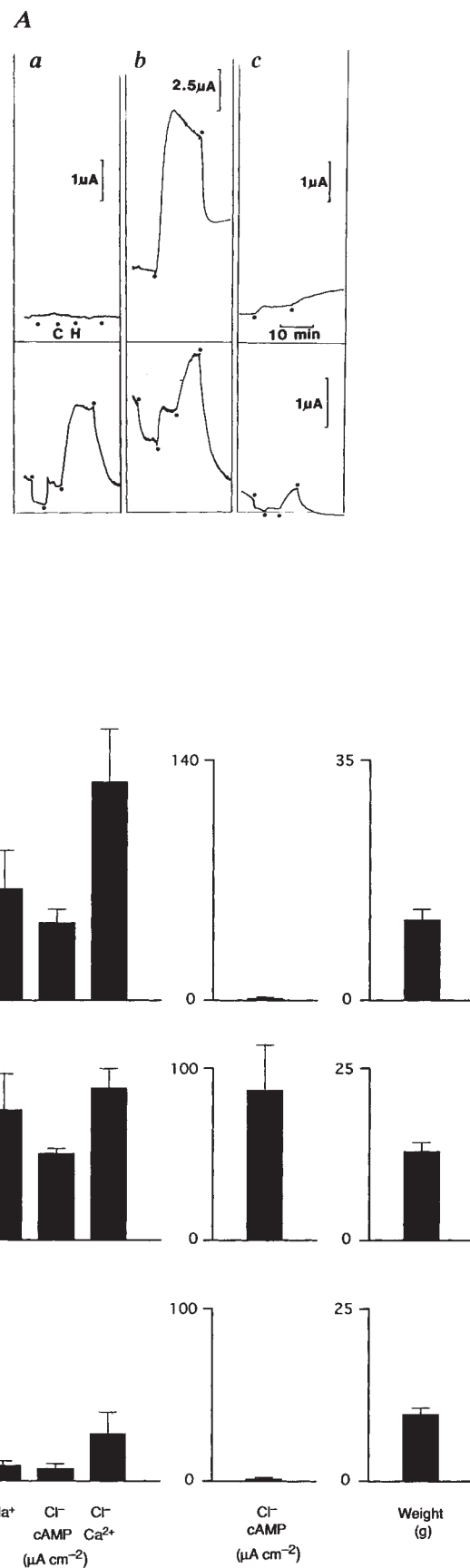


FIG. 3 Detection of human CFTR in different regions of the mouse airway following transfection. Sections from different regions of the airway of a mouse transfected with pREP8-CFTR were hybridized with human antisense *CFTR* probes corresponding to either exons 1–6 (*a–f, i, j*) or exon 13 (*g* and *h*). *a–d*, Expression of human *CFTR* in small and large airways; *e–j*, expression in airspaces in the more distal regions of the lung. Some variation was found in the proportion of cells transfected in different animals which probably reflects differences in the amounts of DNA delivered. Scale bar, 100  $\mu\text{m}$ . See legend to Fig. 2 for details of methods and hybridization probes.

FIG. 4 Correction of the ion channel defects in the trachea of transgenic (*cf/cf*) mice. **A**, Sample traces showing examples of the data from which panel **B** was compiled. Three paired tracheal/caecal preparations are shown. Upper records show measurements for the caecum and lower records for the trachea of the same animal. *a*, *cf/cf* mouse transfected with pREP8-CFTR; *b*, *+/+* mouse transfected with pREP8; *c*, *cf/cf* mouse transfected with the vector pREP8. Four additions were made to each of the tracheal preparations at the time points indicated by dots. First, amiloride (100  $\mu\text{M}$ ) was added (apically) to block electrogenic sodium absorption and to ensure subsequent current increases were not due to this activity.  $\text{EC}_{50}$  for amiloride is  $\sim 1 \mu\text{M}$  and 100  $\mu\text{M}$  will give essentially 100% inhibition<sup>31</sup>. Second, forskolin (10  $\mu\text{M}$ ) was added to both sides of the membrane to stimulate adenylate cyclase and activate cAMP-sensitive chloride channels, increasing chloride secretion. Third, the  $\text{Ca}^{2+}$  ionophore A23187 (1  $\mu\text{M}$ ) was added to both sides of the membrane to activate  $\text{Ca}^{2+}$ -dependent chloride secretion. The ionophore-induced responses were much slower than those induced by forskolin. Finally, frusemide (1 mM) was added basolaterally to block chloride secretion, confirming the nature of the electrogenic transporting activity. Frusemide (1 mM) inhibits over 90% of  $\text{Cl}^-$  secretion<sup>17</sup>. Calibrations for the trachea are the same in each panel. Caecal preparations (upper records) received two additions, forskolin (10  $\mu\text{M}$ , added to both sides of the membrane) and frusemide (1 mM, added basolaterally). Other additions are specifically labelled: C, carbachol (10  $\mu\text{M}$ ); H, histamine (10  $\mu\text{M}$ ). In both the caecum and the trachea the chloride secretory responses were inhibited by frusemide, indicating that they are due to electrogenic chloride secretion from the basolateral to the luminal side of the epithelium. In 8 out of 10 *cf/cf* caeca, frusemide led to a slight increase in short-circuit current (SSC) (*c*, upper record); this is probably due to a blockage of  $\text{K}^+$  secretion and is typical of the caecum of *cf/cf* mice<sup>17</sup>. **B**, Compilation of the data. Mice were subjected to three different treatment protocols: *a*, *cf/cf* mice transfected with pREP8-CFTR; *b*, *+/+* mice transfected with the vector pREP8; *c*, *cf/cf* mice transfected with the vector pREP8. Four animals in each group were matched based on a compromise between weight and age. Data were only included when paired airway and caecal measurements could be made for the same animal. The genotypes of the transfected mice, and of the plasmid DNA with which they were transfected, was unknown at the time the measurements were made. For each treatment regime, three sets of data are shown. (1) The left hand columns show SCC measurements for the trachea. Three measurements of SCC changes are presented:  $\text{Na}^+$ , amiloride-sensitive sodium absorption<sup>31</sup>;  $\text{Cl}^-$  cAMP, SCC change induced by forskolin, presumed to reflect CFTR function<sup>17,32</sup>;  $\text{Cl}^-$   $\text{Ca}^{2+}$ , SCC change induced by the addition of the calcium ionophore A23187. As about 50% of the basal current in the airways was due to sodium absorption, chloride secretion was measured after the addition of amiloride (100  $\mu\text{M}$ ) which abolished electrogenic sodium absorption. (2) The central columns show SCC measurements for the caecum. Only cAMP-sensitive chloride secretion ( $\text{Cl}^-$  cAMP), induced by the addition of forskolin (10  $\mu\text{M}$ ), was measured. Amiloride was not added because the caecum shows no sodium absorptive current<sup>17,33</sup>. (3) The right-hand columns show the weights of the animals used (mean  $\pm$  s.e.m.). Note: the ion transport characteristics of 4/6 pREP8-CFTR transfected *cf/cf* mice were altered by transfection; the reason for the failure of the other two mice is almost certainly failure in delivery. Nevertheless, the forskolin-sensitive SCC ( $\text{Cl}^-$  cAMP) in the whole group including the two failures ( $9.2 \pm 2.6 \mu\text{A cm}^{-2}$ ,  $n=6$ ) was significantly greater ( $P < 0.05$ , Mann and Whitney test) than the value for *cf/cf* mice ( $1.9 \pm 0.5 \mu\text{A cm}^{-2}$ ,  $n=4$ ). Finally, data for two other groups of animals were obtained although these are not illustrated in the figure. Untreated, wild-type (*+/+*) mice ( $n=5$ ; weight  $\pm$  s.e.m. =  $32.2 \pm 2.9$  g) had transport parameters as follows (mean  $\pm$  s.e.m.): for the trachea  $\text{Na}^+$  =  $10.7 \pm 4.8 \mu\text{A cm}^{-2}$ ,  $\text{Cl}^-$  cAMP =  $11.4 \pm 4.3 \mu\text{A cm}^{-2}$ ,  $\text{Cl}^-$   $\text{Ca}^{2+}$  =  $12.1 \pm 4.7 \mu\text{A cm}^{-2}$ ; for the caecum  $\text{Cl}^-$  cAMP =  $35.6 \pm 7.0 \mu\text{A cm}^{-2}$ . Heterozygous (*cf/+*) mice transfected with pREP8-CFTR ( $n=2$ ; mean weight, 7.0 g) had the following transport parameters (mean  $\pm$  s.e.m.): for the trachea:  $\text{Na}^+$  =  $4.5 \mu\text{A cm}^{-2}$ ,  $\text{Cl}^-$  cAMP =  $6.6 \mu\text{A cm}^{-2}$ ,  $\text{Cl}^-$   $\text{Ca}^{2+}$  =  $8.2 \mu\text{A cm}^{-2}$ ; for the caecum  $\text{Cl}^-$  cAMP =  $104.6 \mu\text{A cm}^{-2}$ . Note that the forskolin-sensitive currents ( $\text{Cl}^-$  cAMP) in the trachea were smaller than those reported previously for wild-type mice<sup>17</sup>. This is undoubtedly a consequence of edge damage caused by using only 2.27 mm<sup>2</sup> areas of trachea in the present study, necessitated by the small size of the *cf/cf* mice, compared with 4 mm<sup>2</sup> areas of trachea in previous studies.

**METHODS.** Transgenic mice were genotyped by PCR and/or Southern blot analysis as described<sup>17</sup>. Introduction of plasmid DNA into the mouse airways was as described in the legend to Fig. 2. Trachea and caeca were removed from the transfected animals killed by exposure to 100%  $\text{CO}_2$ . A single tracheal preparation (2.27 mm<sup>2</sup>) and a single caecal preparation (20 mm<sup>2</sup>) was prepared from each animal. The reduction in tracheal area, compared with a previous report<sup>17</sup> was due to the necessity of using animals as small as 5 g. The trachea were cleaned and cut longitudinally along the dorsal



surface and a piece placed under microscopic control in a specially constructed Ussing chamber designed to preserve the curvature of the tissue. Electrogenic ion transport was measured directly as SCC recorded by voltage clamping the tissue at zero potential, as described previously<sup>17</sup>.

compared with the control (+/+) mice, confirming the genotypes of the mice and that the transfection procedure did not affect the gut. Thus, the transfection procedure used can restore CFTR-dependent, cAMP-stimulated chloride secretion by airway epithelia to normal levels.

In the airways of human CF patients there is an increase in amiloride-sensitive sodium absorption, as well as a decrease in chloride secretion, compared with controls<sup>18-20</sup>. It has been suggested that this is crucial to the development of the disease state, as application of amiloride by aerosol alleviates the decline in lung function in CF<sup>21,22</sup>. It is not yet clear how a loss of CFTR function leads to this increase in sodium absorption. In contrast to the human, sodium absorption was reduced in the airways of *cf/cf* mice (Fig. 4B). Transfection of the *cf/cf* mice with pREP8-CFTR, but not with the vector pREP8, significantly increased sodium absorption (seven- to eightfold;  $P < 0.05$ ), to essentially wild-type (+/+) levels (Fig. 4B). Thus, secondary alterations in sodium transport were also corrected to wild-type levels by the transfection protocol used. Finally,  $Ca^{2+}$ -induced chloride secretion reflects an alternative pathway for chloride secretion in the airways distinct from the CFTR pathway<sup>4,23</sup>.  $Ca^{2+}$ -stimulated chloride secretory currents were not defective in *cf/cf* trachea, compared with trachea of normal (+/+) mice, but were significantly increased following transfection with CFTR ( $P < 0.05$ ; Fig. 4B). This latter increase is probably a consequence of hyperpolarization through  $Ca^{2+}$ -sensitive  $K^+$  channels, which increases the electrochemical gradient for  $Cl^-$  exit through the introduced CFTR channels and the pre-existing second pathway<sup>24</sup>.

These data show that the ion transport defects in CF can be corrected *in vivo*. Liposomes, which in clinical trials have been shown to be non-toxic and non-immunogenic, may be safer than viral vectors which have the inherent risks of immunogenicity, replication and transmission. Our results illustrate the invaluable role of transgenic null *cf/cf* mice in assessing the efficiency of various gene therapy approaches. We have shown that functional expression of CFTR not only corrects the primary ion transport defect of the trachea (that is, the cAMP-stimulated chloride secretion), but also corrects secondary alterations in sodium absorption which are a consequence of loss of CFTR function. There seems to be no reason why this approach should not be transferable to humans for the treatment of the pulmonary features of CF. □

Received 4 February; accepted 23 February 1993.

- Riordan, J. R. *et al. Science* **245**, 1066-1073 (1989).
- Anderson, M. P. *et al. Science* **253**, 202-205 (1991).
- Bear, C. E. *et al. Cell* **68**, 809-818 (1992).
- Anderson, M. P. & Welsh, M. J. *Proc. natn. Acad. Sci. U.S.A.* **88**, 6003-6007 (1991).
- Wagner, J. A. *et al. Nature* **349**, 793-796 (1991).
- Chan, H.-C., Goldstein, J. & Nelson, D. J. *Am. J. Physiol.* **262**, C1273-C1283 (1992).
- Snouwaert, J. N. *et al. Science* **257**, 1083-1088 (1992).
- Dorin, J. R. *et al. Nature* **359**, 211-215 (1992).
- Colledge, W. H., Ratcliff, R., Foster, D., Williamson, R. & Evans, M. J. *Lancet* **340**, 680 (1992).
- Yoshimura, K. *et al. Nucleic Acids Res.* **20**, 3233-3240 (1992).
- Stribling, R., Brunette, E., Ligitt, D., Gaensler, K. & Debs, R. *Proc. natn. Acad. Sci. U.S.A.* **89**, 11277-11281 (1992).
- Drumm, *et al. Cell* **62**, 1227-1233 (1990).
- Kartner, N. *et al. Cell* **64**, 681-691 (1991).
- Trezise, A. E. O. & Buchwald, M. *Nature* **353**, 434-437 (1991).
- Trezise, A. E. O. *et al. EMBO J.* **11**, 4291-4303 (1992).
- Trezise, A. E. O., Chambers, J. A., Wardle, C. J., Gould, S. & Harris, A. *Hum. molec. Genet.* (in the press).
- Ratcliff, R. *et al. Nature Genet.* (in the press).
- Boucher, R. C., Stutts, M. J., Knowles, M. R., Cantley, L. & Gatzky, J. T. *J. clin. Invest.* **78**, 1245-1252 (1986).
- Cotton, C. U., Stutts, M. J., Knowles, M. R., Gatzky, J. T. & Boucher, R. C. *J. clin. Invest.* **79**, 80-85 (1987).
- Knowles, M. R. *et al. Science* **221**, 1067-1070 (1983).
- Knowles, M. R. *et al. N. Engl. J. Med.* **322**, 1189-1194 (1990).
- App, E. M. *et al. Am. Rev. resp. Dis.* **141**, 605-612 (1990).
- Williamson, N. J. & Boucher, R. C. *Am. J. Physiol.* **256**, C226-C233 (1989).
- McCann, J. D., Matsuda, J., Garcia, M., Kaczorowski, G. & Welsh, M. J. *Am. J. Physiol.* **258**, L334-L342 (1990).
- Crawford, I. *et al. Proc. natn. Acad. Sci. U.S.A.* **88**, 9262-9266 (1991).
- Zeitlin, P. L. *et al. Proc. natn. Acad. Sci. U.S.A.* **89**, 1344-1347 (1991).
- Cheng, S. H. *et al. Cell* **63**, 827-834 (1990).
- Gregory, R. J. *et al. Nature* **347**, 382-386 (1990).
- Kozak, M. *Cell* **44**, 283-292 (1986).
- Simmons, D. M., Arriza, J. L. & Swanson, L. W. *J. Histochem.* **12**, 169-181 (1989).
- Cuthbert, A. W., Brayden, D. J., Dunne, A., Smyth, R. L. & Wallwork, J. *Br. J. clin. Pharm.* **29**, 227-234 (1990).
- Clarke, L. L. *et al. Science* **257**, 1125-1128 (1992).
- Smith, S. N., Alton, E. W. F. W. & Geddes, D. M. *Clin. Sci.* **82**, 667-672 (1992).

ACKNOWLEDGEMENTS. We thank S. Tucker for advice on the use of the iodide electrode, C. Wardle for advice on western blotting and A. Harris for helpful discussions. A.E.O.T. is a Beit Memorial Fellow. C.F.H. is a Howard Hughes International Research Scholar. This work was funded by the Wellcome Trust, the Cystic Fibrosis Research Trust and the Imperial Cancer Research Fund.

## Germ-line transmission and expression of a human-derived yeast artificial chromosome

Aya Jakobovits, Amy L. Moore, Larry L. Green, German J. Vergara, Catherine E. Maynard-Currie, Harry A. Austin & Sue Klapholz

Cell Genesys Inc., 322 Lakeside Drive, Foster City, California 94404, USA

INTRODUCTION of DNA fragments, hundreds of kilobases in size, into mouse embryonic stem (ES) cells would greatly advance the ability to manipulate the mouse genome. Mice generated from such modified cells would permit investigation of the function and expression of very large or crudely mapped genes. Large DNA molecules cloned into yeast artificial chromosomes (YACs) are stable and genetically manipulable within yeast<sup>1</sup>, suggesting yeast-cell fusion as an ideal method for transferring large DNA segments into mammalian cells. Introduction of YACs into different cell types by this technique has been reported<sup>2-8</sup>; however, the incorporation of yeast DNA along with the YAC has raised doubts as to whether ES cells, modified in this way, would be able to recolonize the mouse germ line<sup>5</sup>. Here we provide, to our knowledge, the first demonstration of germ-line transmission and expression of a large human DNA fragment, introduced into ES cells by fusion with yeast spheroplasts. Proper development was not impaired by the cointegration of a large portion of the yeast genome with the YAC.

Yeast spheroplasts, carrying yHPRT, a 670 kilobase (kb) YAC containing the human hypoxanthine phosphoribosyltransferase (HPRT) gene<sup>4</sup>, were fused with the HPRT-deficient ES cell line E14TG2a (ref. 9). Clones expressing the HPRT locus were selected in hypoxanthine/aminopterin/thymidine (HAT) medium (Fig. 1 legend) and expanded. The human HPRT gene was detected by hybridization in all ES cell clones analysed (not shown). The integration of additional human sequences was examined by comparing the *Alu* profile of 37 HAT-resistant (ESY) clones to that of yHPRT in yeast. Most, if not all, of the 30 *Alu* fragments characteristic of yHPRT were present and of similar relative intensity in over 90% of the ESY clones (Figs 1a, 3B). In clones with an incomplete *Alu* profile (such as ESY 8-5, Fig. 1a) only a few fragments were missing or altered in size. In most ESY clones, the *Alu* pattern appeared to be intact and without significant deletion, rearrangement or segmental amplification.

Integration of YAC vector sequences was investigated with vector arm-specific probes. A 4.5 kb *Hind*III fragment, detected by the right arm probe in yHPRT, was observed in 10 of 20 ESY clones (Fig. 1b). This vector arm was lost in eight ESY clones (for example ESY 3-1, 3-6, Fig. 1b) and rearranged in two (for example ESY 8-6, Fig. 1b). The left arm probe detected the 3 kb and 4.1 kb *Hind*III yHPRT fragments in 18 of 20 clones (Fig. 1c). In total, 8 of the 20 clones (such as ESY 5-2, 8-7, 7-3, Fig. 1a-c) contained complete *Alu* profiles and both intact YAC vector arms.

The structural integrity of yHPRT in ESY clones 5-2 and 8-7 was further evaluated by pulsed-field gel electrophoresis. In yeast carrying yHPRT, five *Sfi*I fragments of the following rough sizes were defined by different probes: 315 kb (*Alu*, left arm),